DEVELOPMENT OF A PERMANENTLY ATTACHED GUIDED ULTRASONIC WAVES ARRAY FOR STRUCTURAL INTEGRITY MONITORING

P.Fromme[1], P. Wilcox[2], M. Lowe[3], and P. Cawley[3]
[1] University College London, UK; [2] University of Bristol, UK; [3] Imperial College London, UK

Abstract: Technical machinery and systems are subject to varying or cyclic service loads and environmental influences, like adverse weather conditions. Such operation conditions can lead to the development of faults during the lifecycle of the structure, e.g., fatigue cracks and severe corrosion damage in offshore oil platforms and oil storage tanks. The corrosion damage often shows as large area thickness reduction in plate-like components of the structure. Guided ultrasonic waves, which propagate along the structure, allow the fast inspection of large areas of a structure from a single sensor location and have a proven performance for the detection of such defects.

A self-contained, permanently attached guided ultrasonic waves array for the constant, long-term monitoring of the structural integrity is being designed and built. The array consists of a ring of piezoelectric transducer elements for excitation and reception of the guided wave. The properties and coupling of the transducers is studied and optimized. The development of the compact array device for the inspection of large areas with minimum power consumption, necessary for long term independent operation, is described. The array operation and data processing schemes are shown. Measurement results are presented and compared to finite element calculations. Good agreement is found and the sensitivity of the guided wave measurement to this kind of defect can be predicted.

Introduction: For the continuous nondestructive monitoring of remote and difficult-to-access structures it would be advantageous to permanently attach monitoring devices that run autonomously, i.e., independent of external energy supply, and transmit data about the condition of the structure wirelessly. An advantage of the permanent attachment of the device to the structure is the possibility of comparative measurements. Taking measurements at different stages in the lifecycle of the structure, an emerging defect can be detected more clearly by comparison to an initial, defect free, measurement, so increasing the sensitivity of the device. Application areas include offshore oil platforms, which are subject to adverse weather conditions, and thus should be inspected regularly for corrosion or the development of cracks. Such structures often consist of large plate-like parts which can be efficiently monitored using guided waves [1,2,3]. Guided waves can propagate over large distances of up to hundreds of meters in one-dimensional structures like pipelines, allowing for an efficient nondestructive testing [4]. In plates the guided waves can propagate in two dimensions. Therefore not only is it necessary to achieve a distinction between the different Lamb wave modes, but the angular resolution of the array also has to be sufficient to distinguish between features in different directions on the structure.

The aim of the project described here is the development of such a permanently attached, autonomous device for monitoring the condition of a large area of plate-like structures from a single position of the device, resulting in a large ratio of the monitored surface to the area occupied by the device. In an array of single transducer elements, ideally each element selectively excites or receives the desired Lamb wave mode in the plate. For an omni-directional inspection of the surrounding plate, the guided wave propagates radially outwards from the excitation source, thus decreasing in amplitude and effectively limiting the inspection range to several meters in a plate.

One of the main issues in the design of such a guided wave array is the angular resolution of signals being reflected at different obstacles lying close to each other, as defects often develop in the vicinity of stress-inducing features like reinforcement bars or connector holes. As pointed out in an earlier contribution [5], it is therefore advantageous to employ only a single mode guided wave to avoid the additional complications of multi-mode guided wave analysis.

Building on a previous study [2], it was decided to employ the A_0 mode below the cut-off frequencies of the higher Lamb wave modes. This mode can be excited efficiently by circular

piezoelectric discs polarized in the thickness direction, applying a vertical force to the plate surface. This results in a flexural wave propagating radially outwards and thus allows an omni-directional inspection of the structure. For the autonomous operation of the device, running on battery power, these excitation transducers can be run with low power consumption. The optimization of the power consumption will be one of the main problems to be resolved in the continuation of this study, to achieve a long battery life. The excitation voltage and number of excitations (number of transducers and averages) must be minimized in order to achieve a desired measurement area and defect resolution with minimum power consumption.

The layout and operation of the guided wave array employed in the preliminary laboratory study is described here. The dynamic range actually achieved with the first prototype was significantly smaller than theoretically predicted. From the evaluation of the measured data, a large amount of coherent noise was found and attributed to problems with the transducer elements employed. A second prototype was therefore designed and results from this are presented.

Results:

Array layout and operation

The preliminary measurements were made on a 5 mm thick aluminum plate (2.45m by 1.25m) in the laboratory. The array layout used in the first prototype consisted of two concentric circles, an outer circle with N_R = 32 receiving elements equally spaced on a diameter of 70 mm, and an inner circle with N_E = 16 excitation elements on a diameter of 50 mm (Fig. 1). Separating the receiving and excitation elements allows for simpler measurement electronics, as all the signals can be acquired in pitch-catch mode. The circular array design was introduced to achieve the same performance in all directions. The setup shown in Fig. 2 was used, employing standard excitation and measurement devices. The excitation signal was a 5 cycle toneburst with a center frequency of 160 kHz modulated by a Hanning window. Multiplexing units were used to switch between the different excitation and receiving transducers. A time trace containing 10000 points was stored for each combination of excitation and receiving transducer. The time traces were measured using a digital oscilloscope with a sampling frequency of 5 MHz. 20 averages were taken and the signal was then transferred to a PC for analysis.
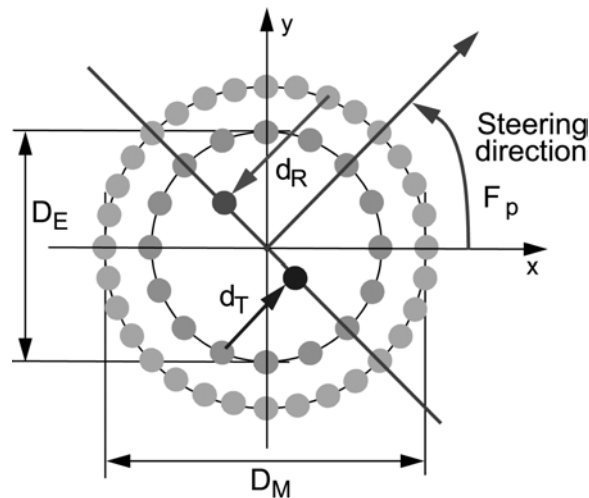

Fig. 1. Array layout, two concentric circles, 32 receiving elements, D_R = 70 mm, 16 excitation elements, D_E = 50 mm; steering direction and path length correction for phased addition algorithm shown.

The number of elements used is limited by the number of channels in the multiplexing unit and the time and power consumption allowed for a single measurement. The maximum element spacing relative to the wavelength at the design frequency should not exceed half the wavelength, to avoid grating lobes. This limits the maximum diameter of the array for a given number of elements, and thus the angular performance of the array, as a larger array will have a better angular resolution and smaller side lobes [6].
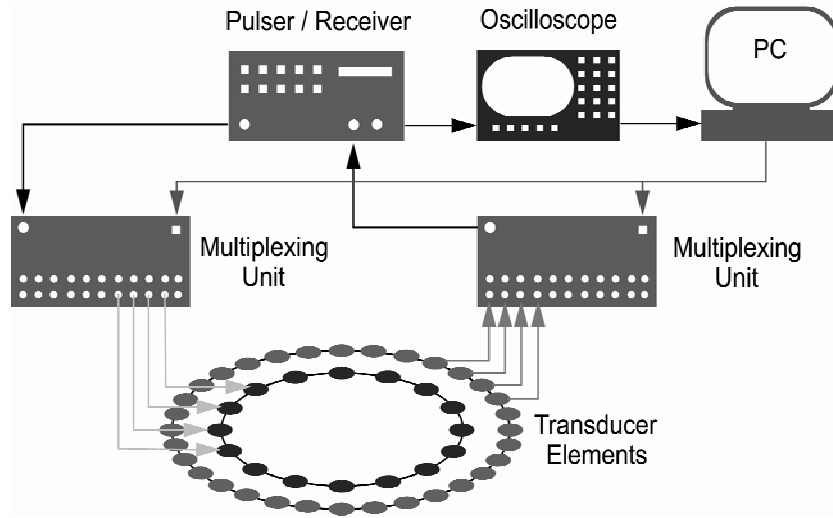

Fig. 2. Schematic view of the experimental setup used for the preliminary laboratory measurements.

The data processing is done in the wavenumber domain, providing effective dispersion compensation [7]. Taking the Fourier transform of each time trace x_i and employing the known dispersion relation for the plate, the wavenumber spectrum X_i is calculated, i.e., the complex magnitude dependent on the wavenumber. A phased addition algorithm is used to synthesize a guided wave beam that can be steered in any direction from the array (Fig. 1). For each of the N_Φ equi-spaced beam steering directions Φ_p the correlation between the $N_E \cdot N_R$ time traces for a guided wave propagating in that direction and being reflected back from the same direction is calculated. To simulate all transducers lying on a line perpendicular to the steering direction, a phase shift is added to each phase spectrum, correcting for the different path lengths (see Fig. 1)

$$d_p = d_R + d_T .$$ (1)

The correlation is calculated by summing the phase spectra for each wave number k

$$A_p(k) = \sum_{i}^{N_E N_R} X_i(k) \cdot \exp(ikd_p) .$$ (2)

The data is then Fourier transformed to the angular order domain and a deconvolution algorithm applied, which improves the angular selectivity of the array significantly. The results are converted back by means of an inverse two-dimensional Fourier transform to obtain an omni-directional B-scan in the radial-angular domain. The data analysis is described in more detail in Ref. [6].

By applying the deconvolution algorithm, the same angular selectivity can be achieved with fewer transducer elements than with a completely filled array. With the available number of elements and a maximum spacing of half the wavelength at the design frequency of 160 kHz, the theoretically achievable angular performance for a signal reflected back from the 0° direction

shows a main lobe that drops to -30 dB at 18°; beyond that the theoretical dynamic range of the array layout is better than 40 dB, which would allow good defect resolution.

First prototype

First measurements were done on an aluminum plate, directly attaching the transducer elements to the plate using a thin layer of two-component conductive epoxy and using standard laboratory equipment as described above. The resulting omni-directional B-scan for the undamaged plate is shown in Fig. 3a, with the position of the array and the plate edges marked. The amplitude is normalized to the maximum reflection (occurring at the closest plate edge) and shown on a grayscale down to −15 dB, the dynamic range of the array prototype being limited by coherent noise in the measured time traces. The measurement shows the reflections of the guided wave at the four sides and the four corners of the plate. The plate edges are only seen in the direction where they are normal to the waves propagating radially from the array. The data processing algorithm is designed to pass signals transmitted and received along the same radial line and to reject signals from other directions.

An artificial model defect was introduced into the plate by drilling a through hole with a diameter of 30 mm at a distance of 0.36 m from the sensor, marked in Fig. 3b. The scattering of the guided wave at such a model defect can be calculated and measured [8]. An additional reflected signal from that defect is visible with an amplitude about 12 dB lower than the maximum reflection at the plate edge. This allows the detection of such a model defect, but care must be taken in the interpretation of these B-scans, as is evident when looking at the same B-scan on a 20 dB scale in Fig. 3c. Here other reflection signals are visible at about −17 dB, which are well above the theoretically predicted dynamic range of −40 dB and might be accidentally interpreted as defects. However they are due to problems with the transducer elements, namely the unwanted excitation and measurement of the S_0 mode. Such a ghost reflection can be seen between the array and the upper edge of the plate, at a position corresponding to the faster propagation velocity of the S_0 mode (marked as "Ghost"). Further problems encountered with this prototype were reverberations of the excited wave at the other transducer elements in the densely populated region of the array. This led to the time signals showing not only the expected single pulse propagating radially outwards from the piezoelectric disc, but overlaid smaller signals from the reverberations. These two effects led to a significant level of coherent noise in the measured signals, which can be reduced by improving the coupling properties between the transducer elements and the structure.

However, as the array is permanently attached to the structure, it is possible to compare current measurements to previous results and to search for changes in the reflection signature of that structure. This is shown in Fig. 3d, where the difference in amplitude between the measurements on the undamaged and damaged plate is plotted relative to the main reflection at the side of the plate. The defect signal is seen very clearly with the larger dynamic range, which is only limited by changes from one measurement to another. It is interesting that the defect not only produces a signal due to the direct reflection of part of the incident wave back towards the device, but also changes the reflection from the plate corner behind the defect. The incident wave is scattered at the defect, thus reducing the energy of the wave reflected at the plate corner behind the defect.
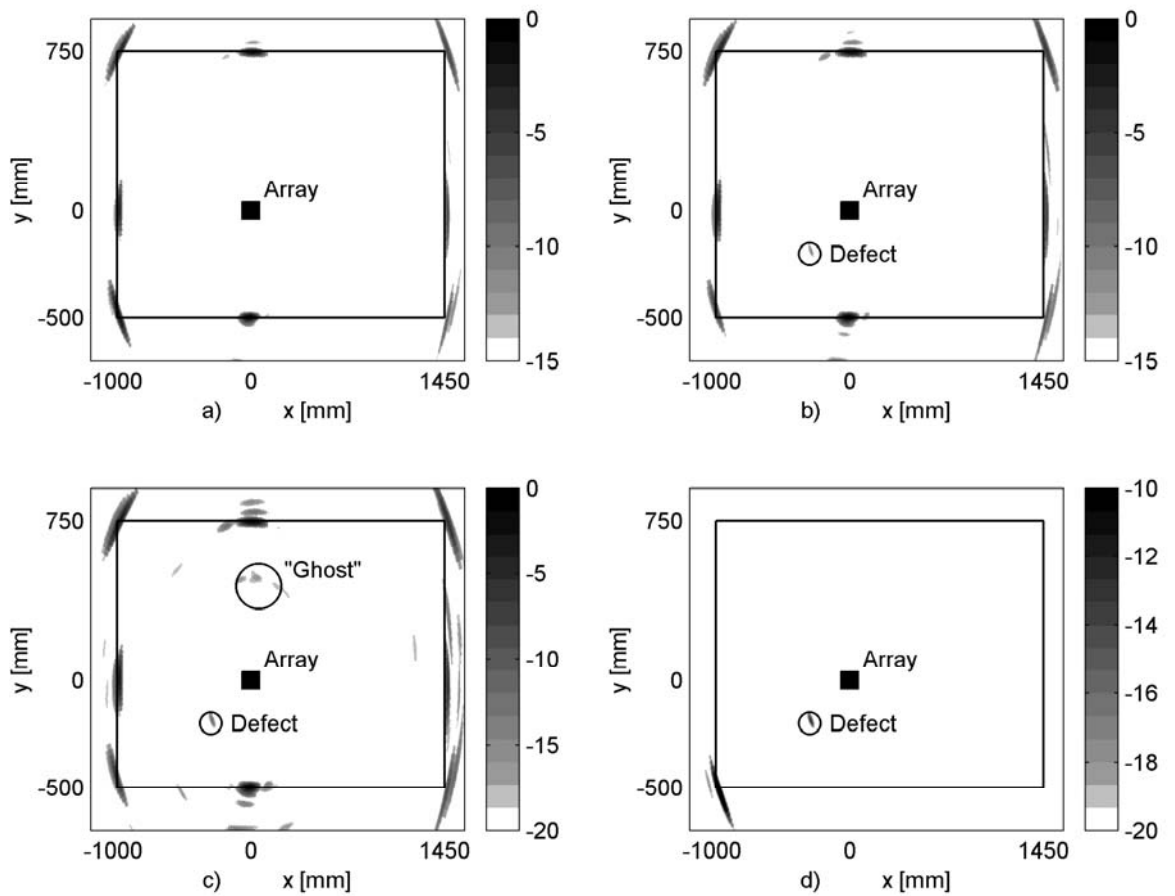
Fig 3. Radial-angular B-scan of plate (edges marked) from shown array position, grayscale representing the correlation of signals reflected, center frequency 160 kHz; a) measurement without defect, 15 dB scale; b) measurement with defect (through hole, r = 15 mm), 15 dB scale; c) measurement with defect (through hole, r = 15 mm), 20 dB scale; d) measured difference due to defect (through hole, r = 15 mm), 20 dB scale.
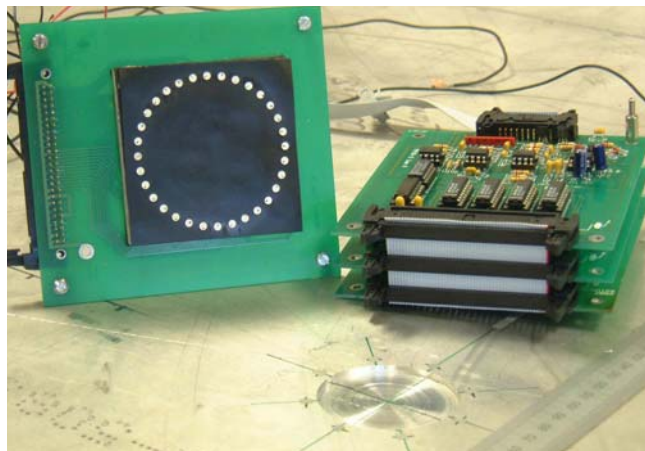

Fig. 4. Second prototype and multiplexing electronics unit on aluminum plate.

Second prototype

The second prototype is shown in Fig. 4, together with the developed multiplexing electronics. This design uses a single ring of elements operating as both transmitters and receivers to reduce problems with inter-element reflections. The generation and reception of the S_0 mode was reduced by bonding a thin conducting membrane between the elements and the structure; this also simplified the construction of the system since it could be assembled away from the plate, rather than the individual elements being attached directly to the plate as in the first prototype. Results from this array on a 5 mm thick, 2450 x 1250 mm aluminum plate are shown in Fig 5. Three steel masses (ca. 30 mm diameter) were bonded to the plate in order to simulate defects. Fig. 5 shows only the quarter of the plate with the simulated defects; the array position is shown as a square and the simulated defects by circles. Clear, distinct reflections can be seen from the three simulated defects and from the edges and corner of the plate. In this case the signal to coherent noise ratio approached 30 dB, so the array performance is a considerable improvement on the first prototype.
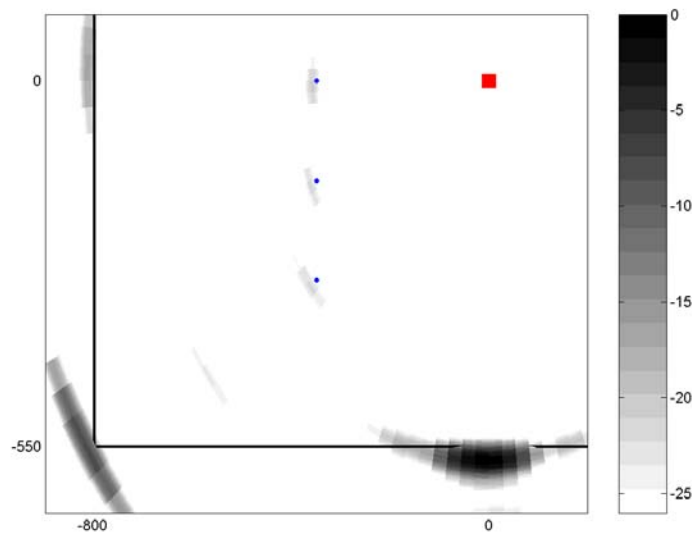

Fig. 5. Radial-angular B-scan of lower left quarter of plate (edges marked) with 3 steel masses glued to plate (circles) from shown array position (square), grayscale representing the amplitude of reflected signals, center frequency 160 kHz, 26 dB scale.

Discussion: Finite Element (FE) calculations of the guided wave propagation and scattering in an isotropic, homogeneous plate were computed using the FINEL code at Imperial College London, UK [9]. Corrosion defects were modeled as part-through circular holes with different diameter and thickness loss (Fig. 6). The same excitation as in the experiments described above was employed. Explicit time integration was used, and the element size and time step were picked to adhere to the usual stability criteria. The FE computations and data analysis are described in more detail in Ref. [10]. The calculated amplitude field was compared to laboratory measurements using a laser interferometer. Good agreement between the calculated and measured amplitude distribution was found, validating the accuracy of the FEM calculations.

The incident antisymmetric guided wave mode (Lamb wave mode A_0) has a given distribution of stresses and displacements through the thickness of the undamaged plate. When the wave hits the damaged area of reduced thickness, the wave propagation is disturbed and part of the energy is scattered. As the defect is not symmetric in respect to the plate thickness, mode conversion occurs (usually corrosion occurs only on one side of the structure). The scattered waves also contain symmetric guided wave modes (Lamb wave modes S_0, SH) besides localized vibrations around

the defect. Part of the energy propagates along the area of reduced thickness, and secondary scattering occurs at the far end of the defect. These wave pulses overlap in time and can lead to a higher or lower received signal in different directions, depending on the phase lag. A significant influence of this interference is evident, as the amplitude ratio varies for different geometries and excitation frequencies. This could pose problems for practical testing applications, as the defect size and depth are not known a priori and several defects of different severity can occur in a structure. Therefore in real-life testing, measurements should be performed using a pulse with a relatively broad frequency bandwidth and evaluated over a range of frequencies.

For the evaluation of the sensitivity of the guided wave array, the amplitude of the backscattered A_0 mode pulse is of special interest, as this is the quantity measurable at the location of the array device. Therefore the amplitude of this pulse was monitored halfway between the excitation source and the defect (0.2 m from the hole center) and the ratio between the amplitudes of the incident wave pulse and backscattered wave pulse investigated. For the defect size and excitation frequency of interest in this study, calculations were done for a variation of the defect depth, modeling the material loss due to corrosion of different severity. The calculated amplitude ratios of the backscattered pulse compared to the incident pulse were calculated for a defect of 30 mm diameter and 25%, 50%, and 75% material loss. The maximum reflected amplitude varies significantly with the thickness reduction. For the same normalization with the incident wave, maximum amplitude ratios of 0.03   (-30dB) for 25% thickness reduction, 0.1 (-20dB) for 50% thickness reduction, and 0.2 (-14dB) for 75% thickness reduction were observed. Therefore the sensitivity to very shallow defects of only a few percent localized thickness reduction (corrosion pitting) is rather limited. However, the method should also be rather robust to normally occurring thickness variations in the structure. The predicted maximum amplitude of the backscattered wave pulse for severe defects is significant, and well within the dynamic range of the second array prototype. This should allow the detection of such severe corrosion defects over large distances in plate-like structures.
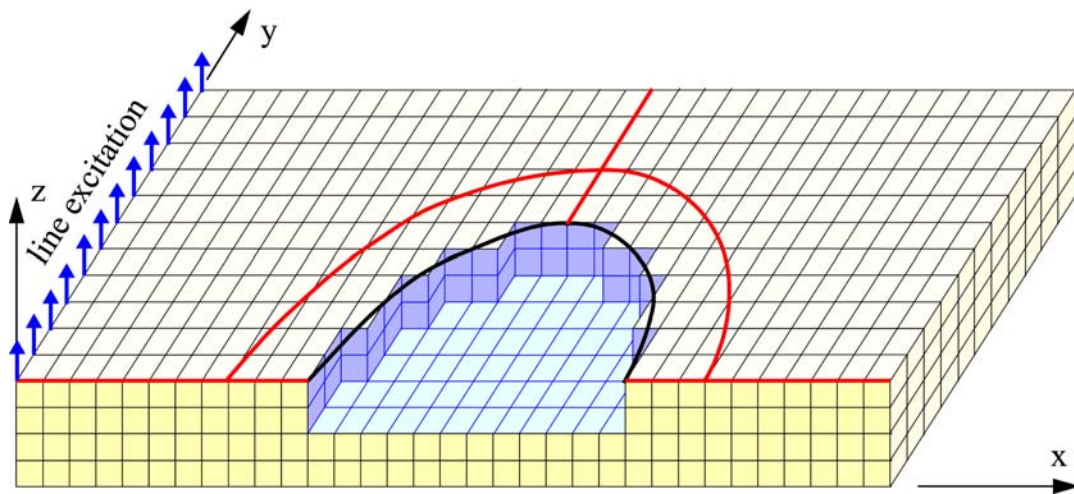

Fig. 6. Schematic of the three-dimensional model for finite element calculations.

Conclusions: Two prototypes of a guided wave array for the permanent monitoring of plate-like structures have been designed and tested. The first antisymmetric Lamb wave mode A_0 is excited and measured using piezoelectric transducer elements. Preliminary measurements with the prototypes and standard laboratory measurement equipment were made on an aluminum plate. The first array had a signal to coherent noise ratio of –15 dB, significantly smaller than the theoretically predicted dynamic range of –40 dB. The main sources of coherent noise were the

unintended excitation of the S_0 mode and reverberations of the excited wave pulse at the other transducer elements in the densely populated area of the array. Improvements to the dynamic range of the device were therefore needed for the reliable detection of small defects.

The second prototype reduced the number of piezoelectric elements in the array by using the same elements for excitation and reception; this significantly reduced inter-element reflections. A thin conductive membrane between the elements and the test plate improved the ratio of the generated and received A_0 mode components compared to S_0 and gave a further signal to coherent noise improvement. This second prototype gave a signal to coherent noise ratio approaching 30 dB which is useful for the detection of typical corrosion defects.

Finite element modeling of the reflection and scattering of guided waves at simplified corrosion defects was performed. Good agreement with laboratory experiments was found, allowing the use of the numerical modeling to study the sensitivity of the measurement method for the detection of corrosion damage. The predicted reflected amplitude levels lie well within the dynamic range of the second prototype, with a strong dependence on the amount of material loss (thickness reduction), allowing for a good detection of severe defects.

References:

1. Fromme, P. and Sayir, M.B., in *Rev. Prog. QNDE,* Vol. **20B**, ed. by D.O. Thompson and D.E. Chimenti, AIP Conference Proceedings 557, New York, 1626-1633 (2001).
2. Wilcox, P., Lowe, M.J.S., and Cawley, P., in *Rev. Prog. QNDE,* Vol. **19A**, *op. cit.*, AIP Conference Proceedings 509, New York, 1049-1056 (2000).
3. Malyarenko, E.V. and Hinders, M.K., *J. Acoust. Soc. Am.* **108(4)**, 1631-1639 (2000).
4. Alleyne, D.N., Pavlakovic, B., Lowe, M.J.S., and Cawley, P., *Insight* **43(2)**, 93-96 (2001).
5. Alleyne, D.N. and Cawley, P., *NDT & E Int.* **25(1)**, 11-22 (1992).
6. Wilcox, P., in *Rev. Prog. QNDE,* Vol. **22A**, *op. cit.*, AIP Conference Proceedings 657, New York, 761-768 (2003).
7. Wilcox, P., Lowe, M.J.S., and Cawley, P., in *Rev. Prog. QNDE,* Vol. **20A**, *op. cit.*, AIP Conference Proceedings 557, New York, 555-562 (2001).
8. Fromme, P. and Sayir, M.B., *J. Acoust. Soc. Am.* **111(3)**, 1165-1170 (2002).
9. Hitchings, D., "FE77 User manual", Imperial College London, UK.
10. Fromme, P., Wilcox, P., Lowe, M., and Cawley, P., in *Rev. Prog. QNDE,* Vol. **23A**, *op. cit.*, AIP Conference Proceedings 700, New York, 142-149 (2004).